©Freund Publishing House Ltd., International Journal of Nonlinear Sciences & Numerical Simulation 11(10): 777-784, 2010

Numerical and Experimental Study on Dielectrophoretic and Electrohydrodynamic Traps using Micro-Particles on an Interdigitated Electrode Array System

Tae-Woo Lee[1], Kihawn Nam[1], Sang-Hyun Baek[1], Woo-Jin Chang[2], Sun-Kook Kim[3], Han-Sung Kim[1], Dae-Sung Yoon[1], and Sang Woo Lee[1,*]

[1]*Department of Biomedical Engineering, Yonsei University, Wonju, Gangwondo, 220-710, Korea*

[2]*Micro Nanotechnology Laboratory, University of Illinois at Urbana-Champaign, 208 North Wright Street, Urbana, Illinois, 61801, USA*

[3]*Samsung Advanced Institute of Technology, Mt. 14-1, Nongseo-doing, Giheung-gu, Yongin-Si, Gyeonggi-do, Republic of Korea*

Abstract

Dielectrophoretic and electrohydrodynamic traps are presented that can localize microparticles on specified positions of an interdigitated electrode array. For the generation of the traps, an interdigitated electrode array chip covered by an oxide layer with 10 μm x 10 μm opening windows is designed and fabricated, then an AC signal with varying frequency is applied to the array, the traps are finally created on the positions between two opening windows or inside the windows by dielectrophoretic and electrohydrodynamic effects. In addition, the dielectrophoretic and electrohydrodynamic forces are analyzed numerically using a finite element method.

Keywords: Dielectrophoreis (DEP), electrothermal force, AC electroosmotics, Indterdigiated Electrode, Micro-particles

1. Introduction

Dielectrophoresis (DEP)-based traps for localization of micro-/nano-scale objects on microelectrode structures have been intensively studied by many researchers. Micro-/nano-particles and micro-electronic devices have been trapped on a specific region of microelectrode structures using DEP force [1-3]. The dielectrophoretic capture of bio-particles such as spores, cells, viruses, and electronic devices has also been demonstrated in a micro-device [4-8]. In additions, while several reagents were added in a monitoring system, each individual bio-particle was trapped in a specific target position by dielectrophoretic force in order to monitor the response of individual bio-particles continuously [9,10]. Most studies mentioned above focused on the traps used with DEP. However, it also should be noted that AC signals applied to microelectrode structures not only produce DEP forces, but also generate electro-hydrodynamic (EHD) forces such as electro-thermal and AC electroosmotic forces [7,11-13]. Ramos et al. [11] and Chen et al. [12] characterized the effects of AC electro-kinetics when AC signal was applied on the micro-electrode. The characteristics of electro-chemical micro-gripper were also investigated with the reduced-order model that allows the nonlinear analysis to perform rapidly [13]. These EHD forces can also play an important

* Corresponding author:
yusuklee@yonsei.ac.kr (S. W. Lee)

role in the generation of traps for the localization of the micro-/nano-particles in microelectrode structures. Nonetheless, systematic analysis results regarding these forces have not been studied in the previous reports. In this paper, the DEP and EHD traps on an interdigitated electrode array (IDA) system, which can localize a few micro-particles, were designed, and fabricated. Using the structure, the 5.47 μm polystyrene beads were trapped on specific isolated positions. In addition, DEP, electrothermal, AC electroosmotic forces creating the traps on the IDA system were analyzed using the finite element method. The dielectrophoretic and electrohydrodynamic traps for the localization of micro-particles on the interdigitaed array electrode system are characterized through the comparison between the experimental results and the numerical ones.

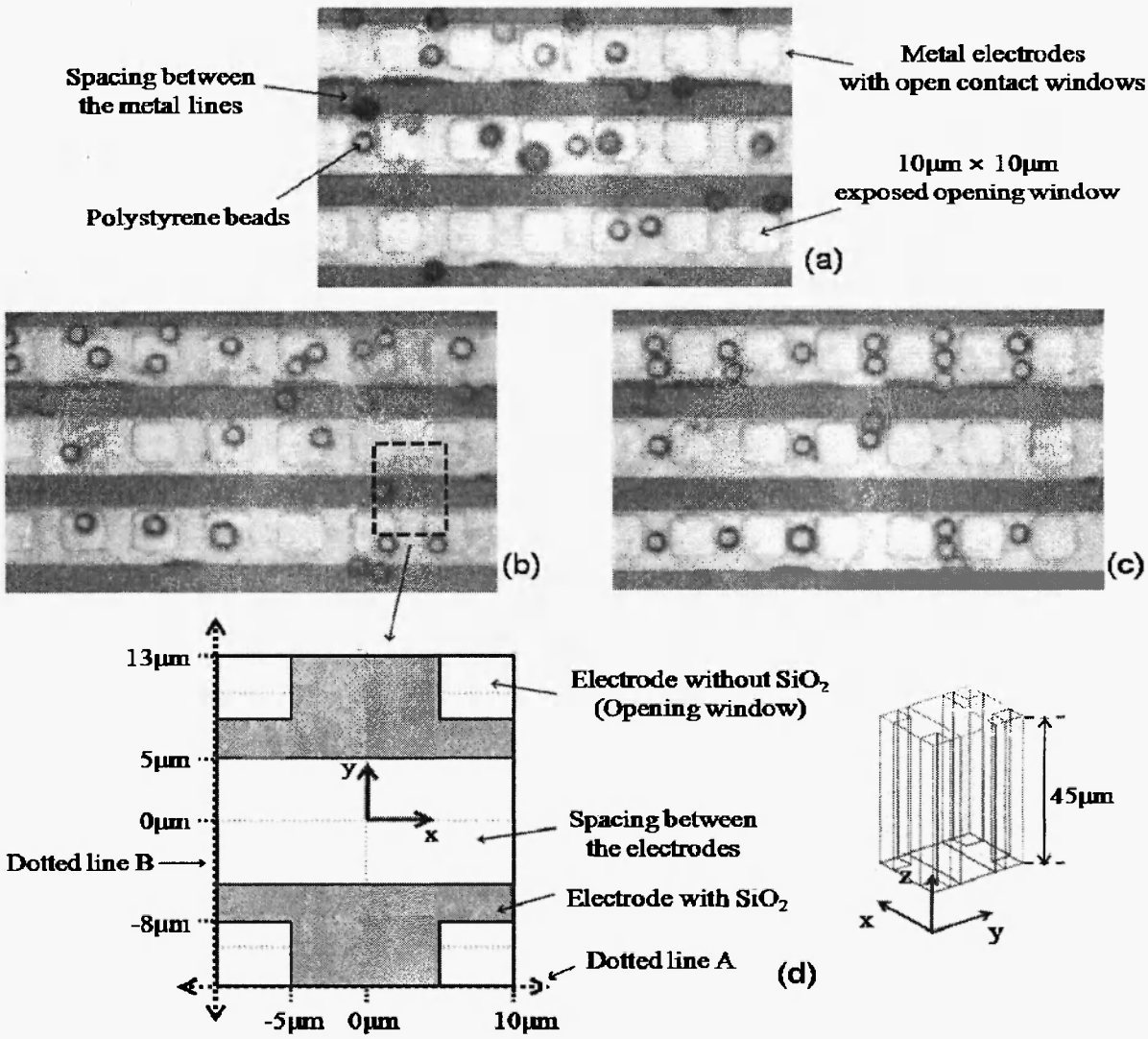

Fig. 1: (a-c) The movements of negatively charged polystyrene beads while the magnitude and the frequency of applied AC signal were changed, (a) no bias, (b) 10 V_{p-p} and 1 kHz, (c) 10 V_{p-p} and 10 MHz; (d) the schematic diagram of the interdigitated electrode array system: the two and three-dimensional view of FEM simulation structure for numerical study.

2. Materials and Methods

2.1 Procedures of Experiment

The photolithographic patterns for an IDA having 16 μm width and 10 μm space between the electrodes were defined on a silicon dioxide layer. A chromium layer with 150 Å thickness and a gold layer with 300 Å thickness were sequentially deposited in an E-beam evaporator and patterned using lift-off process. After the deposition of a 3000 Å thick oxide layer in a plasma-enhanced chemical vapor deposition (PECVD) chamber, the photolithographic and wet etching techniques were used for the creation of 10 μm x 10 μm opening windows as shown in Figure 1(a)-(c). For the demonstration of the traps for the localization of micro-particles under DEP electrothermal, and AC electroosmotic forces, 50 μl solution containing 5.47 μm diameter polystyrene beads (Spherotech Inc. Liberty ville, IL, # CP-50-10) coated with carboxyl group were introduced onto the fabricated IDA structure, where the concentration of original stock solution is 1.093 x 10^8 #/ml and the concentration of the solution used for the experiment is 5.465 x 10^5 #/ml by the dilution of dionized (DI) water. A sinusoidal signal with 10V peak-to-peak and varying frequencies was applied using micro-manipulator probes while a silicone rubber ring isolated the probes from the solution at the test sites. The movement of the beads was observed under a microscopy and record using CCD camera.

2.2 Procedures of Numerical Simulation

For the characterization of the experimental results, DEP, electrothermal, and AC electroosmotic effects were investigated by a numerical study. To conduct the numerical investigation, the IDA structure with the same dimensions as in the experiment was generated by finite element method (FEM) software (COMSOL Multiphysics 3.5a). Since the structure of the IDA system is symmetric, the IDA system can be simplified to the region composed of two half electrodes with four quarter opening windows for the numerical study. Figure 1(d) illustrates the schematic diagram of the structure generated to perform the study.

The equations involved in the numerical investigation are as follows: when a particle under electrical field is in a solution, DEP force is represented as [14]

$$F_{DEP} = 2\pi\varepsilon_m r^3 \,\mathrm{Re}(f_{cm})\nabla|E|^2 \qquad (1)$$

where r, ε_m, and E are the radius of the particle, the real permittivity of the medium, and the electric field, respectively. The Clausius-Mossotti (CM) factor, f_{cm}, is $\dfrac{\tilde{\varepsilon}_p - \tilde{\varepsilon}_m}{\tilde{\varepsilon}_p + 2\tilde{\varepsilon}_n}$, where $\tilde{\varepsilon}_p = \varepsilon_p - j\dfrac{\sigma_p}{\omega}$ and $\tilde{\varepsilon}_m = \varepsilon_m - j\dfrac{\sigma_m}{\omega}$ are the complex permittivities of the solution and particles, σ_m, ε_p, σ_p, and ω represent the real conductivity of the solution, the real permittivity of the particle, the real conductivity of the particle, the angular frequency, respectively.

AC electrothermal effect on a fluid is related to the time-averaged electric force density by spatial variations of electrical conductivity and permittivity due to the local temperature gradient. The time-averaged electric force density is described as [11]

$$< F_e >= -0.5\left(\frac{\nabla\sigma_m}{\sigma_m} - \frac{\nabla\varepsilon_m}{\varepsilon_m}\right)\bullet E\frac{\varepsilon_m E}{1+(\omega\tau)^2} - 0.25|E|^2\nabla\varepsilon_m \qquad (2)$$

where $\tau = \dfrac{\varepsilon_m}{\sigma_m}$ is the charge relaxation time of the solution. In addition, the velocity of the fluid (u) induced by the electric force density can be calculated by the incompressible Navier-Stokes equation [11]

$$\eta\nabla^2 u - \nabla p + < F_e >= 0 \qquad (3)$$

where η and p are the viscosity of a medium and the pressure, respectively. To solve this equation, the mass-conversion equation for the incompressible medium

$$\nabla \bullet u = 0 \tag{4}$$

is also needed.

Lastly, the velocity of the fluid (v_{AC}) generated by AC electroosmotic effect, is given by [15]

$$v_{AC} = \frac{1}{8}\frac{\varepsilon_m V_o^2 \Omega^2}{\eta z(1+\Omega)} \tag{5}$$

$$\Omega = \omega \frac{\varepsilon_m}{\sigma_m}\frac{\pi}{2} z\kappa \tag{6}$$

where V_o is the amplitude of the AC signal applied into an interdigitated electrode array system, z is the distance from the center of space between two electrodes of the IDA system, and κ is the reciprocal Debye length.

In order to characterize the traps for the localization of micro-particles in the IDA system as shown in Figure 1, the equations described above were solved using finite element method (FEM) software according to the following steps:

(i) We generated the data of the electrical field using the electric model [16] when applying AC potential into the IDA system. Using this data, the simulation results of DEP force were calculated by applying the DEP formula into the software.

(ii) The spatial variations of electrical conductivity and permittivity due to a local temperature gradient were calculated by the electric model and heat transfer model [17]. Sequentially, the data the time-averaged electric force densities were extracted by the time-averaged electric force density equation in combination with the data of the electric field and the spatial variations. Finally, the velocity data of the fluid described in the incompressible Navier-Stokes equation was calculated by the laminar flow model [18] using the data of time-averaged electric force density.

(iii) The data of fluidic velocity induced by the AC electroosmotic effect was generated by inserting the AC electroosmotic formula to the FEM Software when applying AC potential into the IDA system.

3. Results and Discussion

According to the observations of the movement of the beads under a microscope, the beads were positioned randomly prior to the signal application. At 1 kHz and 10 $V_{peak\text{-}to\text{-}peak}$, the beads were trapped inside the opening windows. On the other hand, the trap positions for the localization of beads were moved to the middle between the opening windows when the frequency increased to 10 MHz. Figures 1(a)-(c) show these traps as depicted by to the behaviors of the 5.47 μm diameter polystyrene beads on the IDA structure. For the characterization of the experimental results, the DEP, the electrothermal, and the AC electroosmotic effects were investigated through the simulation results. The simulation were performed with the following parameters; the density (1000 kg/m^3), the heat capacity (4184 J/(kg·K)), the dynamic viscosity (0.00108 Pa·s), the relative electrical permittivity ($80.2\varepsilon_o$) and thermal conductivity (0.598 W/(m·K)) of DI water [19]; the thermal conductivity (0.93 W/(m·K)) of the PECVD deposited oxide [20], and the relative electrical permittivity ($2.6\varepsilon_o$) of the polystyrene bead [21]. The measured electrical conductivity of the DI water containing the carboxyl coated beads was 1 x 10^{-6} S/m (Handylab, LF-11, Schott Instrument). The effective electrical conductivity of the bead was 3.2 x 10^{-6} S/m calculated by the following formula [22]

$$\sigma_p = \sigma_b + \frac{2K_s}{r} \tag{7}$$

where σ_b ($\simeq$ 0 S/m), K_s (= 4.48 nS), and r (= 2.74 μm) are the bulk conductivity, the surface conductance, and the radius of the polystyrene bead, respectively.

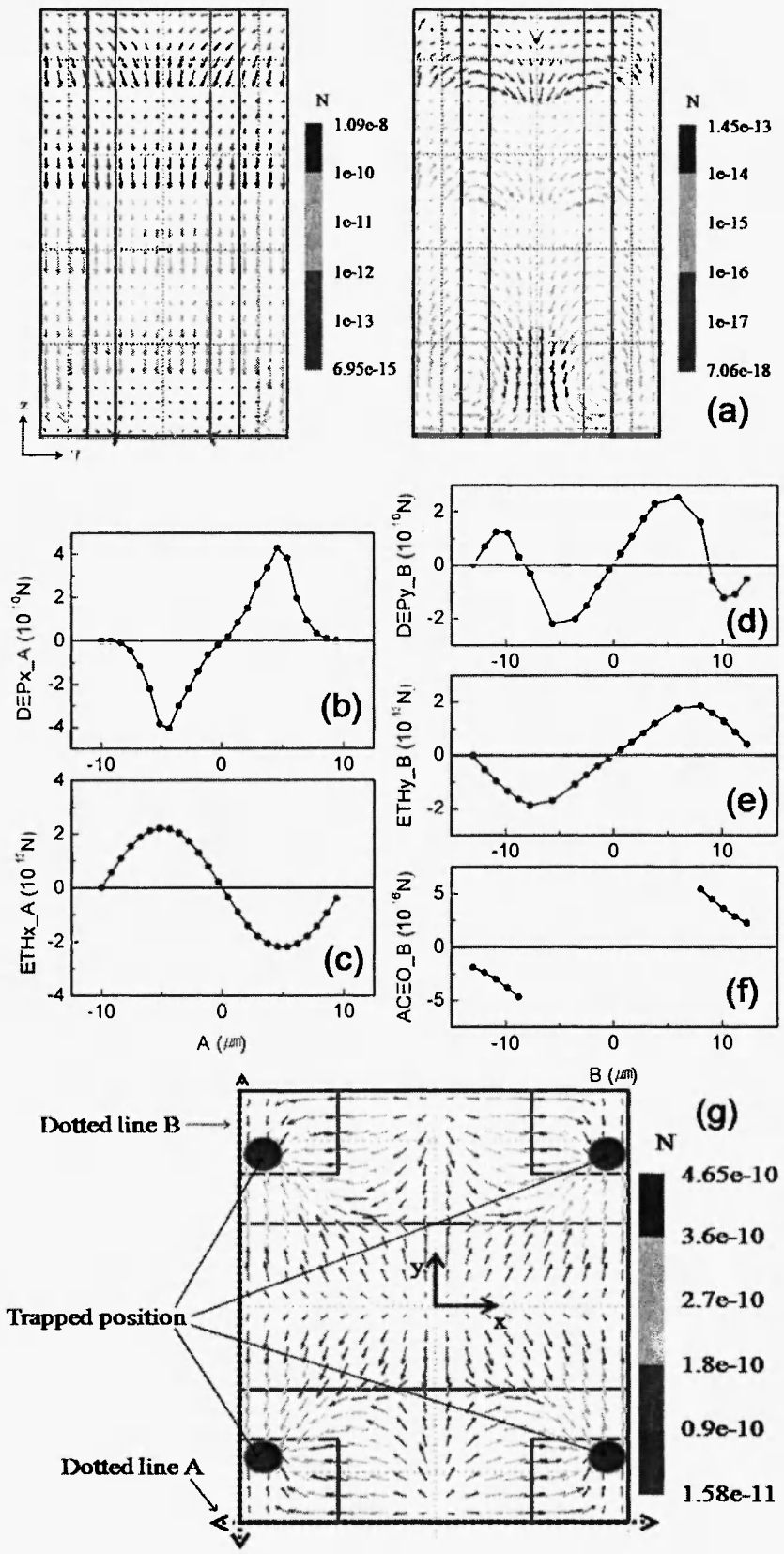

Fig. 2:
(a) The DEP force (left figure) and the electrothermal force (right figure) in the yz-surface, where the AC signal with 1 kHz and 10 $V_{peak\text{-}to\text{-}peak}$ was applied into the IDA structure;
(b-c) The DEP force and the electrothermal force in the x-direction on the dotted line A;
(d-e) the DEP force and the electrothermal force in the y-direction on the dotted line B;
(f) the AC electro-osmotic force on the surface of the IDA structure; (g) the total force field associated with the DEP, the electrothermal, and the AC electro-osmotic forces acting on the beads in the xy-surface at a height of 2.74 μm, where the applied voltage and frequency are $10V_{p\text{-}p}$ and 1kHz.

At 10 $V_{peak\text{-}to\text{-}peak}$ and 1 kHz, the z component of the DEP and the electrothermal forces acting on the 5.48 μm diameter bead is downward to the surface of the IDA structure, as shown in Figure 2(a). Thus, the beads should be contacted on the surface, where the center of the bead is located at 2.74 μm from the surface. At the low frequency, AC electroosmotic effect is generated by the tangential component of the electric field above the diffuse layer on the electrodes of the IDA structure. Considering the shape of the IDA structure shown in Figure 1(d), the tangential component of the electric field is directed to the center onto the electrode, resulting in the direction of the AC electroosmotic force being toward the center of the electrodes [11] Hence, the DEP, electrothermal, and AC electroosmotic forces acting on the beads contacted on the surface decide the position of the traps when applying AC signal 10 $V_{peak\text{-}to\text{-}peak}$ and 1 kHz in the IDA structure. Figures 2(b)-(f) show these forces in the x-direction or the y-direction. The beads located on the dotted line A are moved toward the opening windows, according to Figures 2(b)-(c). In additions, Figures 2(d)-(f) demonstrate that the beads located on the dotted line B are also moved inside the position of the opening windows in the y-direction. More generally, the total force field associated with the DEP, the AC electroosmotic and the electrothermal forces acting on the beads at the 2.74 μm height converges into the opening windows, as shown in Figure 2(g). As a result, the traps are created inside the opening windows. These numerical simulation results are in close agreement of the experimental results shown in Figure 1(b).

At 10 $V_{peak\text{-}to\text{-}peak}$ and 10 MHz, there are no AC electroosmotic effects [11] Hence, only the DEP and electrothermal forces are evaluated at that frequency. Moreover, the z-component of the DEP and electrothermal forces, which move the beads upward, are reduced as increasing the height (z-direction) from the IDA structure, as shown in Figure 3(a). It is also noted that gravity moving the beads downward acts on the bead. Therefore, the equilibrium height that the bead is stationary in z-direction should be firstly found in order to recognize the traps of the given particles. The total force associated with the DEP force, the electrothermal force and gravity in z-direction is zero around 37μm from the electrodes, as shown in Figure 3(b). At that height, the total force field of the DEP and the electrothermal forces in xy-surface illustrates in Figure 3(d). Since the y-axis component of total force field is much greater than the x-axis component, the force vectors consisting of the force field seem to be vertical, as shown in Figure 3(d). However, the x-axis component of the total force field also exists. For example, Figure 3(c) represents the x-axis component of it when the beads located on the dotted line A. Therefore, the beads distributed randomly at the equilibrium height are rapidly moved to the center of the electrodes (e.g: the dotted line A), according to Figure 3(d). Subsequently, the collected beads on the dotted line A are slowly moved and trapped to the position between two opening windows by the weak force shown in Figure 3(c). Those simulation results are well matched to the experimental results in Figures 1(c). Moreover, the simulation and experiment results, as shown in Figure 1-3, suggest that the position of the localized traps can be controlled by varying the amplitude and frequency of applied AC signal.

4. Conclusion

In conclusion, we constructed the two-dimensional traps on the IDA structure with the 10 μm x 10 μm opening windows for the localization of micro-/nano-particles using dielectrophoretic, electrothermal and AC electroosmotic effects. The traps were experimentally verified by the localization of 5.47 μm polystyrene beads on the specific sites. Moreover, the characterization of the traps generated by the DEP, the electrothermal, and the AC electroosmotic effects were investigated through the numerical simulation. The results revealed that changing electrode structure (e.g. opening windows), frequency and amplitude of the applied signal could easily control the trap positions of the given particles.

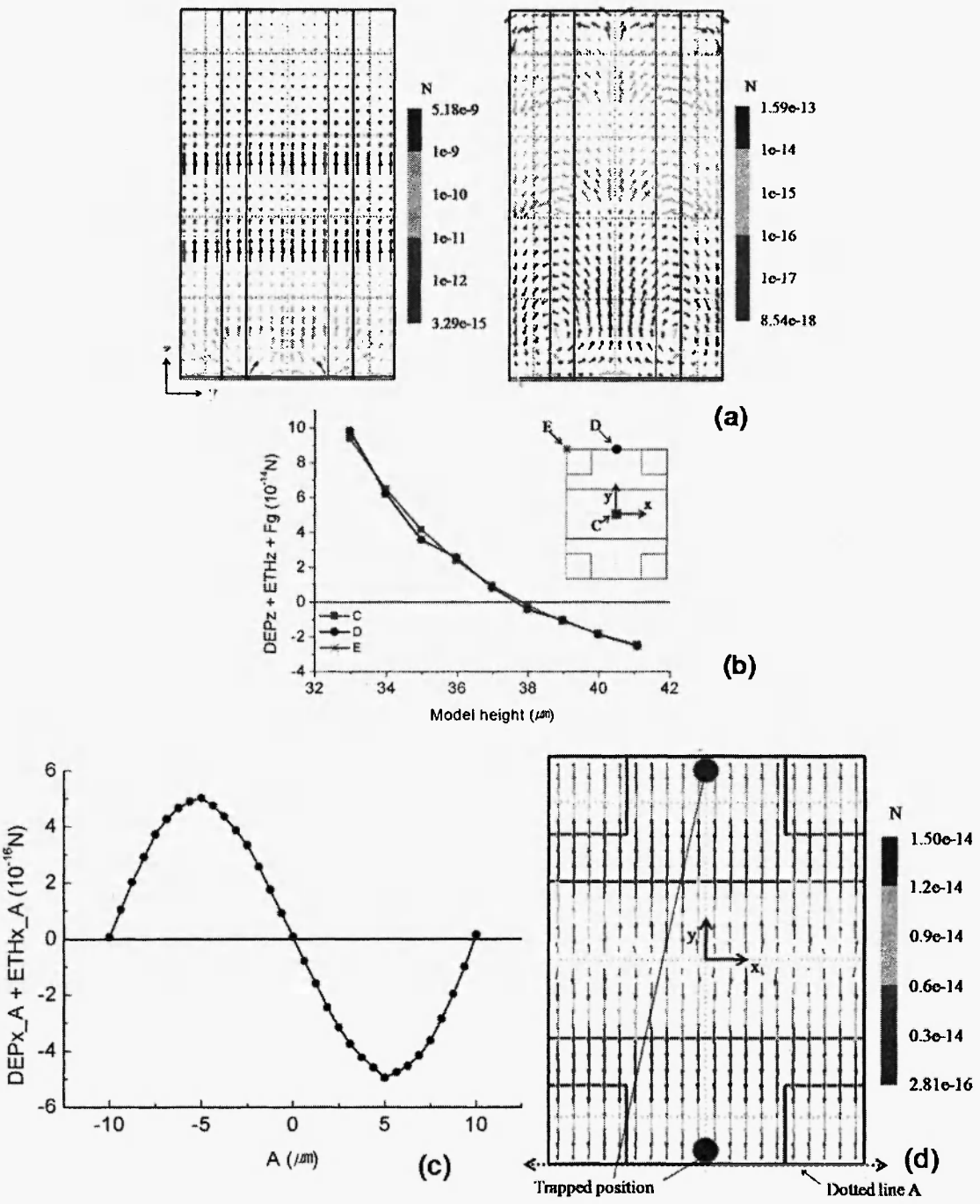

Fig. 3: (a) the DEP force (left figure) and the electrothermal force (right figure) in the yz-surface, where the AC signal with 10 MHz and 10 $V_{peak\text{-}to\text{-}peak}$ was applied into the IDA structure (b) The summation of the negative DEP force, the electrothermal force and the gravity at C, D, or E position in the z-direction, where the inset figure shows the top view of the IDA structure and the positions; (c) the force acting on the bead located on the dotted line A in the x-direction; (d) the total force field acting on the bead located on the xy-surface at the equilibrium height of 37 μm, where the applied voltage and frequency are $10V_{p\text{-}p}$ and 10MHz.

Acknowledgements

This research was supported in part by National Research Foundation of Korea (NRF) under Grant No. 2010-0013619, 2009-0068841, KRF-2007-313-D00963 and KRF-2008-313-D00580, R01-2008-000-11338-0.

References

[1] Green NG., Morgan H. Dielectrophoretic separation of nano-particle, *J. Phys. D.*, **30**(1997), L41-L44

[2] Green NG, Morgan H. Separation of submicrometre particles using a combination of dielectrophoretic and electrohydrodynamic forces, *J. Phys.* D., **31**(1998), L25-L30

[3] Lee SW, Bashir R. Dielectrophoesis and Chemically Mediated Directed Self-Assembly of Micrometer-Scale Three-Terminal Metal Oxide Semiconductor Field-Effect Transistors, *Adv. Mater.*, **17**(2005), 2671-2677

[4] Morgan H, Hughes MP, Green NG. Separation of Bioparticles by Dielectrophoresis, *Biophys. J.*, **77**(1999), 516-525

[5] Liu YS, et al. Electrical Detection of Germination of Model Bacillus Anthracis Spores in Microfluidic Biochips, *Lab. Chip*, 7(2007), 603 – 610

[6] Park K, Akin D, Bashir R. Electrical Capture and Lysing of Viruses in Silicon Nanoprobe Array, *Biomed. Microdevice.*, **9**(2007), 877-883

[7] Islam N, Lian M, Wu J. Enhancing microcantilever capability with integrated AC electroosmotic trapping, *Microfluidics and Nanofluidics*, **3**(2007), 369-375

[8] Park K, Jang J, Irimia D, Sturgis J, Lee J, Robinson JP, Toner M, Bashir R, Living cantilever arrays' for characterization of mass of single live cells in fluids, *Lab Chip*, **8**(2008), 1034-1041

[9] Liu YS, et al. Assembly of Single Cells Arrays Using Image Dielectrophoresis *The 14th Int., Conf., on Solid-State Sens., Actuat., Microsys.*, Lyon, France, 473-476 (2007)

[10] Voldman J, Braff RA, Toner M, Gray ML, Schmidt M. A. Holding Forces of Single-Particle Dielectrophoretic Traps, *Biophys. J.*, **80**(2001), 531-541

[11] Ramos A, Morgan H, Green NG, Castellanos A., AC electrokinetics: a review of forces in microelectrode structures, *J. Physics D*, **31**(1998), 2338-2353

[12] Chen DF, Du H. Simulation studies on electrothermal fluid flow induced in a dielectrophoretic microelectrode system, *J. Micromech. Microeng.*, **16**(2006), 2411-2419,

[13] Chu JK, Guan L, Qi DZ, et al.Rapid Nonlinear Analysis for Electrothermal Microgripper Using Reduced Order Model Based on Krylov Subspace, Int. J. Nonlin. Sci. Num., **9**(2008), 333-338

[14] Pohl HA. *Dielectraphoresis*, Cambridge University Press, Cambridge, UK (1978)

[15] Ramos A, Morgan H, Green NG, Castellanos A., AC Electric-Field Induced Fluid Flow in Microelectrodes, *J. Coll. Inter. Sci.*, **217**(1999), 420-422

[16] COMSOL Inc., *COMSOL MANUAL, AC/DC Module User Guide Chapter 4.* COMSOL Inc., Sweden (2008)

[17] COMSOL Inc., *COMSOL MANUAL, Heat Transfer Module User Guide Chapter 2,* COMSOL Inc., Sweden) (2008)

[18] COMSOL Inc., *COMSOL MANUAL, MEMS Module User Guide Chapter 8*, COMSOL Inc., Sweden (2008)

[19] Lide DR. *CRC Handbook of Chemistry and Physics, 79th Edition*, CRC Press, Boca Raton, FL., USA (1998)

[20] Haflzovic S, Paul O. Temperature-dependent thermal conductivites of CMOS Layers by micromachined thermal van der Pauw test Structures, *Sens. & Actuat. A*, **97-98**(2002), 246-252

[21] Chang DK. *Field and Wave Electromagnetics, 2nd Edition*, Addison-Wesley Publishing Com., New York, USA (1999)

[22] Hughes MP et al., The Dielectrophoretic Behavior of Submicron Latex Spheres: Influence of Surface Conductance, *J. Colloid Interf. Sci.*, **220**(1999), 454-457